Rapid Detection of Adulteration in Minced Lamb Meat Using Vis-NIR Reflectance Spectroscopy

Xiaojia Zuo [1], Yanlei Li [2,*], Xinwen Chen [1], Li Chen [3] and Chang Liu [2]

[1] Xinjiang Laboratory of Animal Products Quality and Safety, Institution of Animal Husbandry Quality Standards, Xinjiang Academy of Animal Science, Urumqi 830011, China; zuoxj85@126.com (X.Z.); 2021001691@bgy.edu.cn (X.C.)

[2] School of Mechanical and Electrical Engineering, Beijing Polytechnic College, Beijing 100042, China; 15690518186@163.com

[3] Institute of Food Science and Technology, Chinese Academy of Agricultural Sciences, Beijing 100193, China; chenliwork@126.com

* Correspondence: liyanlei2021@163.com; Tel.: +86-15600985511

Abstract: In view of the phenomenon that adulterated lamb with other animal-derived meats in the market could not be quickly identified, this study used visible near-infrared spectroscopy combined with chemometric methods to quickly identify and quantify lamb rolls adulterated with chicken, duck, and pork. The spectra of the visible–near-infrared band (350–1000 nm) and near-infrared band (1000–1700 nm) of 360 lamb samples, which were mixed with chicken, duck, pork, and 10% lamb oil separately in different increasing proportions, were collected. It was found that the qualitative models of heterogeneous meat (adulterated with chicken, duck, and pork) in lamb were constructed by the combination of first derivative and multiplicative scatter correction (MSC); the accuracy of the validation set reached 100%; the meantime accuracy of the cross-validation set reached 100% (pure lamb), 98.3% (adulterated with chicken), 98.7% (adulterated with duck), and 97.3% (adulterated with pork). Furthermore, the correlation coefficient (R^2c) of the adulterated chicken, pork, and duck quantitative prediction models reached 0.972 (chicken), 0.981 (pork), and 0.985 (duck). In summary, the use of Vis NIR can identify lamb meat mixed with chicken, duck, and pork and can quantitatively predict the content of adulterated meat.

Keywords: visible and near-infrared reflectance spectroscopy; adulterated lamb; qualitative identification; quantitative prediction; partial least squares discrimination analysis

1. Introduction

With the improvement in people's living standards and the transformation of consumption concepts, the diet structure has become more diversified, and food safety awareness has grown stronger. The foundation of food safety assurance is the identification of food authenticity. According to the data released by the National Bureau of Statistics of China, the proportion of meat consumption in residents' diet has been increasing year by year recently, especially lamb with high nutritional value, which is increasingly favored by consumers. In 2021, the lamb production in China was 5.14 million tons, while apparent consumption was about 5.55 million tons, and the per capita consumption was 3.93 kg, which is an increase of 4.93% from 2020 [1]. With the increase in lamb per capita consumption year by year, illegal businessmen, in order to reduce costs and seek higher profits, make fake lamb through various forms, disrupting the market [2]. Taking advantage of the fact that consumers do not have the ability to identify fake mutton, presenting inferior products as superior, they violate the interests of consumers and disrupt the market order [3,4]. Therefore, it is urgent to develop a fast and non-destructive testing method to check the quality of meat products.

At present, the methods used for the meat origin identification of adulterated meat mainly include PCR [5,6], ELISA [7,8], mass spectrometry [9–11], and near-infrared spec-

troscopy [12–15]. Although the first three methods can follow national standards and international standards [16,17], they all need to use large-scale instruments for qualitative and quantitative identification, which limits their application scope. Near-infrared spectroscopy (NIR) is a mature qualitative and quantitative analysis technology, which can collect information on the structure and composition of samples [18] by detecting the frequency doubling and sum frequency of C-H, N-H, O-H, and other hydrogen-containing groups. It can analyze multiple components and parameters at the same time and has the advantages of high efficiency, fast speed, low cost, non-destructive testing, and environmental protection, which have attracted many researchers to apply it in the identification of adulterated meat in recent years [19–22]. Dixit et al. [23] used a near-infrared spectroscopy model to identify adulterated pork and lamb in beef, and the identification accuracy could reach 100% after standard normal variance and de-trend preprocessing. Savoia et al. [24] further identified beef and lamb adulterated with pork, chicken, and horse meat by near-infrared spectroscopy and modeling by partial least squares qualitative discrimination (PLS-DA). The results indicated that when the adulterated beef and lamb were less than 10%, the prediction ability of the model still had good accuracy, and the resolution of the verification set could reach 78.95–100% for the prediction of different proportions of adulterated meat. Many researchers further expanded the wavelength range to obtain more information and improve the qualitative and quantitative accuracy [25–27]. For example, Weng et al. [28] used reflection spectrum modeling in a visible–near-infrared band between 300 and 2500 nm to identify the types and adulteration amount of pork or viscera in ground beef, and the model prediction set recognition rate of adulteration meat types could reach 99.0%. Furthermore, to expand the wavelength range, Alamprese [3] used UV–visible, NIR, and MIR spectroscopy to detect minced beef adulteration with turkey by the partial least squares (PLS) modeling method, which showed that the qualitative and quantitative effects of NIR and MIR on adulterated turkey were better than those of UV–visible.

Compared with the existing literature, this study significantly improves the quantitative prediction accuracy of different types of adulterated components in lamb meat by optimizing the spectral acquisition interval and adopting advanced mathematical preprocessing methods based on near-infrared spectroscopy analysis. The constructed model can not only identify whether other meats are adulterated in lamb meat but also accurately identify the types of adulterated meats. In order to accelerate the industrial application of NIR spectroscopy technology, application costs should be reduced by shortening the wavelength range under the premise of ensuring the accuracy of the model as much as possible. With this purpose, two portable NIR devices were used in this study to collect the spectral information of 350–1000 nm and 1000–1700 nm spectra, comparing the result of visible–shortwave NIR and NIR identification models. Using the features of the wavelength range instead of the wavelength point method for screening the optimal bands, lamb/non-lamb qualitative identification models, identification models of adulteration meat type (chicken, duck, and pork), and quantitative prediction models of adulterated components were built to quickly identify adulterated mutton with the purpose of providing technical support for practical application in industry.

2. Materials and Methods

2.1. Sample Preparation

The sheep thick flank meat, pork tenderloin, chicken breast, duck leg, and sheep fat used in the experiment were purchased from Beijing Hualian Supermarket. The purchased meats were trimmed to remove surface fat, fascia, and epidermis. They were then cut into 3 cm × 3 cm pieces and ground into minced meat using a meat mincer (QSJ-C04K3, Bear Electric Appliance Co., Ltd., Foshan, China) for subsequent use. Additionally, sheep oil, with the blood portion removed, was cut into small pieces, twisted into sludge and set aside for utilization. Chicken, duck, pork, and 10% sheep fat were individually incorporated into minced lamb, adhering to the SBT11093-2014 standard [29] for central reserve frozen rolled lamb. The precise proportions of these ingredients are outlined in Table 1. The mixture

was thoroughly blended to ensure that the proportions of the adulterated meat (chicken, duck, or pork) were accurately represented at 0%, 10%, 30%, 50%, 70%, and 90% within the samples. The prepared samples were placed into sample bags, put into the meat box mold (180 mm × 80 mm × 40 mm), pressed, and frozen in a −20 °C refrigerator. After 8 h, the samples were removed, vacuum-sealed to form square bricks, and then frozen at −20 °C for 48 h.

Table 1. Summary of meat mixtures prepared.

Mixture Type	Group	Proportion of Chicken/Duck/Pork (%)	Proportion of Lamb (%)	Proportion of Lamb Fat (%)
Lamb mixed with chicken	0% Chicken/Pure lamb	0	90	10
	10% Chicken	10	80	10
	30% Chicken	30	60	10
	50% Chicken	50	40	10
	70% Chicken	70	20	10
	90% Chicken	90	0	10
Lamb mixed with duck	0% Duck/Pure lamb	0	90	10
	10% Duck	10	80	10
	30% Duck	30	60	10
	50% Duck	50	40	10
	70% Duck	70	20	10
	90% Duck	90	0	10
Lamb mixed with pork	0% Pork/Pure lamb	0	90	10
	10% Pork	10	80	10
	30% Pork	30	60	10
	50% Pork	50	40	10
	70% Pork	70	20	10
	90% Pork	90	0	10

2.2. Spectra Acquisition

The frozen square bricks were slightly melted and placed on the slicer (BQPJ-I, Aibo Stainless Steel Mechanical Engineering Co., Ltd., Jiaxing, China). They were then cut into 1 mm thick slices and laid flat on a table with a black background for collection.

The portable spectrometer (Detector: AvaSpec-2048x14; band: 350–1000 nm; spectral resolution: 0.05 nm; Avantes, Apeldoorn, The Netherlands; Self-built large area annular light source: 20 W halogen tungsten lamp reflector cup) and handheld spectrometer (Detector: MicroNIR; band: 900–1700 nm; Double-integrated vacuum tungsten light source; JDSU, Milpitas, CA, USA) were used to collect the spectral data of 350–1000 nm and 900–1700 nm bands of samples, which were collected in real time with the AvaSoft 8.7 and MicroNIR 1.5.7 software of the instruments.

Before collection, the spectrometer was preheated for 20 min, and the black-and-white reference correction was performed on the spectrum acquisition system. The collection parameters were set as follows: for the portable spectrometer (band range: 350–1000 nm; integration time: 100 ms, average number: 5); for the handheld spectrometer (band range: 900–1700 nm, integration time: 38 ms, scanning times: 50). The reflectance spectrum data from three different sites were collected for each sample, and the average spectrum was calculated as the representative spectrum of the sample. Due to the high noise signal in the spectral information 900–1000 nm from the handheld spectrometer, the 900–1000 nm band was removed, and the more stable 1000–1700 nm band was retained.

2.3. Spectral Data Preprocessing

The acquisition of original spectral data often involves unavoidable interference, such as ambient light reflection. To minimize the impact of noise and irrelevant information on modeling, it is crucial to employ appropriate mathematical processing methods for preprocessing the original spectral data. This preprocessing step is vital for eliminating in-

terference factors in the spectral data, enhancing the precision and stability of the predictive model [30].

In this study, we utilized several preprocessing techniques, including the first derivative, second derivative, multiplicative scatter correction (MSC), and standard normal variate (SNV), to improve the stability of the constructed model. The first derivative processing technique is primarily used to eliminate baseline offsets in the original spectrum, which can distort the true shape of the spectral peaks. By applying the first derivative, we can obtain a more accurate representation of the spectral features. The second derivative processing method helps to separate overlapping peaks and emphasize peak characteristics, making it easier to identify distinct spectral signatures. MSC is employed to correct for variations in scattering caused by differences in particle size and surface roughness. This technique ensures that the spectral data are more representative of the actual chemical composition of the samples rather than being influenced by physical factors. Similar to MSC, SNV is used to normalize the spectral data by removing the effects of non-uniform scattering interference. It achieves this by scaling the spectral data such that the mean is zero and the variance is one for each sample [31,32]. The choice of these preprocessing methods was based on their ability to enhance the quality of the spectral data and, consequently, improve the predictive power of the models.

2.4. Near-Infrared Model Development

For the development of the lamb/non-lamb qualitative identification model, a total of 360 samples were randomly divided into two subsets: a calibration set comprising 270 samples and a prediction set containing 90 samples, adhering to a ratio of 3:1. Specifically, the calibration set served to train the model, whereas the prediction set was utilized to assess its performance. In machine learning and statistical modeling, it is usually recommended to divide the data set into a calibration set and a prediction set to evaluate the model's generalization ability. The 3:1 ratio is a common method as it provides sufficient data to train the model while also having a considerable amount of data to validate the model's predictive ability. The 3:1 ratio is to strike a balance between the bias and variance of the model. If the prediction set is too small, the model may overfit, resulting in poor generalization ability on unseen data. On the contrary, if the calibration set is too small, the model may underfit and fail to capture key patterns in the data [33,34].

Similarly, for the identification models of adulterated meat types (chicken, duck, and pork), 120 samples were allocated per model with 90 samples in the calibration set and 30 samples in the validation set. This division enabled the development and subsequent validation of models capable of distinguishing between pure lamb and lamb adulterated with chicken, duck, or pork. The calibration set samples were used to construct the quantitative analysis model, and the prediction set samples were used to validate and evaluate the model's performance. The qualitative model was constructed using partial least squares discriminant analysis (PLSDA), which was developed based on PLSR. PLSDA matrices refer to the category information of the samples in the form of codes, applying linear statistical modeling of spectral information with the categories and finding a certain number of principal factors that most accurately characterize the original data set; therefore, the qualitative discriminant models built are more effective and have efficient discriminatory capability [30,31]. The quantitative model was constructed using the partial least squares regression analysis (PLSR) method, which is the most widely used in NIR spectral analysis as a representative of linear correction methods that maximize the correlation between the spectral data and the parameters to be quantified [14,35].

2.5. Model Evaluation

The performance evaluation of the model focuses on accuracy, stability and predictive ability. The main qualitative model evaluation parameters are Root Mean Square Error of Calibration (RMSEC), Root Mean Square Error of Prediction (RMSEP), Sensitivity and Specificity, as well as Root Mean Square Error of Cross-Validation (RMSECV). In addition,

quantitative model evaluation parameters mainly include the correction set correlation coefficient (Rc), prediction set correlation coefficient (Rp), RMSEC and RMSEP. Sensitivity is the rate at which the group of samples can be correctly identified. Specifically, specificity is the accuracy of identifying samples that are not in the group. These two parameters can be calculated by the following formula:

$$\text{Sensitivity} = \frac{\text{IT}}{\text{IT} + \text{UT}} \tag{1}$$

$$\text{Specificity} = \frac{\text{IF}}{\text{IF} + \text{UF}} \tag{2}$$

where IT (Identified True) is the number of samples belonging to this class and identified; UT (Unidentified True) is the number of samples belonging to this class and unidentified; IF (Identified False) is the number of samples unbelonging to this class and identified; and UF (Unidentified False) is the number of samples unbelonging to this class and unidentified.

2.6. Data Processing

All data analysis and model building are performed using MATLAB R2014a (MathWorks, Inc., Natick, MA, USA) with PLS Toolbox 9.3.1 (Eigenvector Research Company, Wenatchee, WA, USA).

3. Results and Discussion

3.1. Original Spectral Analysis of Adulterated Meat with Different Proportions in Two Bands

To ensure consistency and minimize variability, the spectra of 20 repeated samples were averaged for each meat type to obtain representative spectra, which were then used to analyze group differences in this study. Among them, the samples with 0% adulteration of chicken, duck, and pork represent the lamb group, and the samples with 90% adulteration of chicken, duck, and pork are considered as pure chicken, duck, and pork groups, respectively. The representative NIR spectra of the chicken, duck, pork and lamb groups in the two bands of 350–1000 nm and 1000–1700 nm are shown in Figure 1.
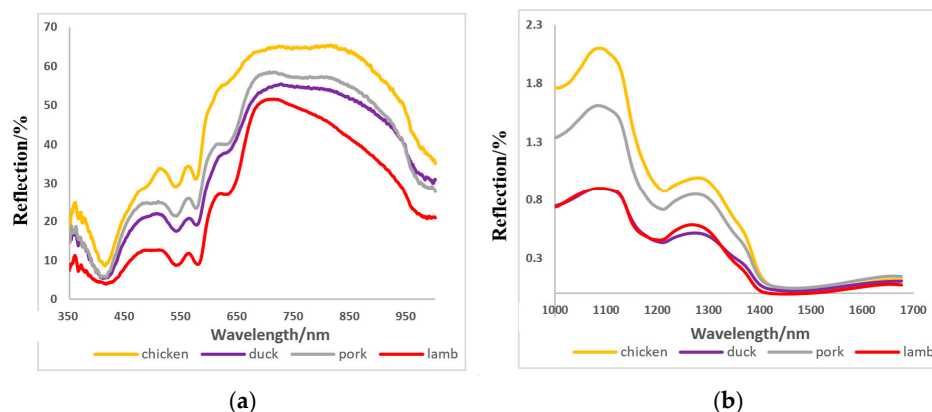

(**a**)   (**b**)

Figure 1. The near infrared spectra of chicken, duck, pork and lamb. (**a**) The near infrared spectra of chicken, duck, pork and lamb in 350–1000 nm wavelength, (**b**) the near infrared spectra of chicken, duck, pork and lamb in 1000–1700 nm wavelength.

Reflectance intensities across the 350–1000 nm and 1000–1700 nm bands varied among species with a notable decrease from chicken to lamb. The minimal variations between lamb and duck/pork are attributed to species-specific pigmentation and matrix composition, which significantly influence the NIR reflectance patterns [36,37]. The relation for spectral region and chemical compound is displayed in Table 2. The NIR spectra of lamb adulterated with varying proportions of chicken, duck, and pork across two bands (350–1000 nm and 1000–1700 nm) are presented in Figures 2 and 3. Reflectance ratio in-

tensities showed a general trend of convergence toward that of the adulterating meat with the most pronounced changes observed in the 1000–1700 nm band. Species-specific myoglobin contents and protein compositions contribute to the distinct NIR reflectance patterns with less pronounced correlations observed for duck and pork adulteration in the 1000–1700 nm band compared to chicken [38,39]. Notably, the 1080 nm peak, associated with N-H bonds, showed pronounced changes with varying adulteration levels, highlighting protein composition discrepancies between species, which is the same as the findings of Kademi et al. [40].

Table 2. Relation for spectral region and chemical compound.

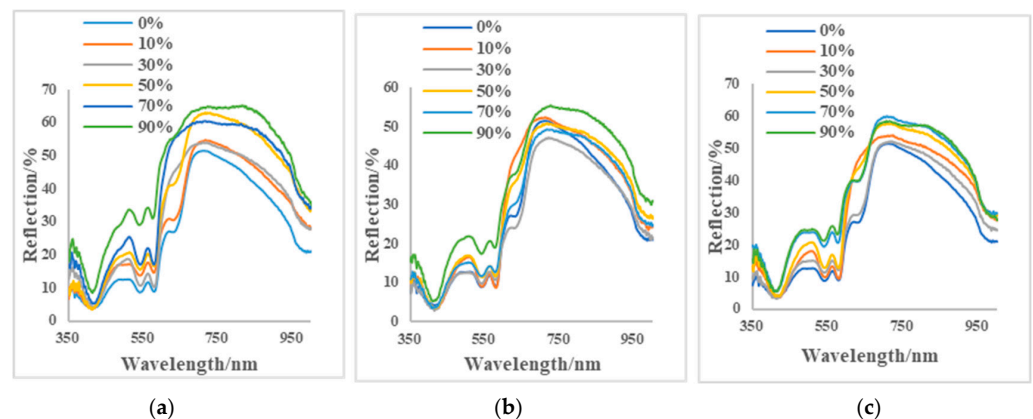| Spectral Region (nm)	Primary Absorbing Species/Chemical Bonds	Chemical Substances Description
430	Absorption bond related to myoglobin	Reflects trace amounts of myoglobin
574	Absorption of oxymyoglobin	Reflects the content of oxymyoglobin
630	Absorption of metmyoglobin	Reflects the content of metmyoglobin
1000–1200	Vibrational absorption of C-H, N-H bonds	Reflects protein variability information
1450	Overtone absorption of O-H bonds	Reflects water composition
1080	N-H bond	Reflects protein differences

(a) (b) (c)

Figure 2. The near-infrared spectra of lamb adulterated with different proportions of chicken, duck and pork in 350–1000 nm wavelength. (**a**) Lamb adulterated with different proportions of chicken; (**b**) lamb adulterated with different proportions of duck; (**c**) lamb adulterated with different proportions of pork.
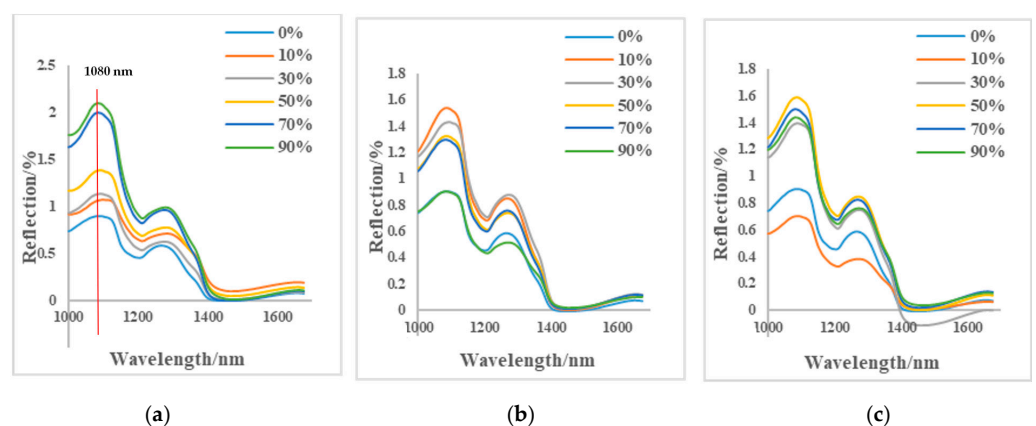

(a) (b) (c)

Figure 3. The near-infrared spectra of lamb adulterated with different proportions of chicken, duck and pork in 1000–1700 nm wavelength. (**a**) Lamb adulterated with different proportions of chicken; (**b**) lamb adulterated with different proportions of duck; (**c**) lamb adulterated with different proportions of pork.

3.2. Screening of Characteristic Wavelength Ranges

The NIR spectra were analyzed over specific intervals designed to retain valid spectral information and minimize noise. Samples, categorized into pure lamb and adulterated groups with varying percentages of chicken, duck, and pork, underwent a 5-point smoothing pre-treatment prior to PLSDA model construction [39].

Cross-validation confirmed the stability and predictive accuracy of our models, particularly within the 400–1000 nm and 1000–1400 nm bands where RMSECV values were minimized. It can be observed from Table 3 that the RMSECV of the model in the visible-NIR band is smaller than that in the NIR band as a whole, and the model constructed in the visible-NIR band in the 400–1000 nm band has the highest stability with an RMSECV of 0.172; the model constructed in the NIR band in the 1000–1400 nm band has the highest stability with an RMSECV of 0.232. The specificity of the pure lamb group in the validation set indicates the recognition accuracy of non-lamb samples with values closer to 1 indicating better discrimination between pure and adulterated lamb. The optimal band of NIR is 1000–1400 nm, the sensitivity values of chicken adulterated, duck adulterated and pork adulterated are 100%, 83.3%, 95.8%, respectively. By comparing the modeling results obtained by the stepwise regression analysis method, it was found that the sensitivity of the lamb group and specificity of the adulterated group were both lower than the models constructed by the characteristic wavelength ranges screening method at 350–1000 nm and 1000–1700 nm, while the RMSECV was higher. Further analysis shows that four fifths of the 25 characteristic wavelength points screened by stepwise regression analysis method from 350 to 1000 nm are in the optimal wavelength range of 400–1000 nm, and 12 of the 13 characteristic wavelength points screened from 1000 to 1700 nm are in the optimal wavelength range of 1000–1400 nm, which proves that the characteristic wavelength data are also effectively screened by the characteristic wavelength ranges screening method, and the model built in this way has better accuracy. Therefore, the subsequent study will further examine modeling and optimization based on these two bands, respectively, and the optimal solution to solve this research problem will be obtained.

Table 3. Comparison of model parameters in different wavelength ranges.

Method	Wavelength Range (nm)	Factor Number	RMSECV	Sensitivity of Lamb Adulterated with Others (%)			
				Pure Lamb	Chicken	Duck	Pork
Feature Band Selection	350–1000	11	0.186	98.6	84.2	100	96.0
	450–1000	**12**	**0.172**	**98.6**	**100**	**100**	**100**
	550–1000	12	0.182	100	94.7	100	96.0
	650–1000	13	0.205	98.6	100	100	100
	750–1000	15	0.214	94.2	89.5	72.0	88.0
	1000–1700	17	0.242	98.5	100	79.2	95.8
	1000–1600	16	0.234	98.5	100	79.2	95.8
	1000–1500	16	0.237	98.5	100	83.3	95.8
	1000–1400	**14**	**0.232**	**98.5**	**100**	**83.3**	**95.8**
	1000–1300	14	0.237	100	100	87.5	87.5
Stepwise Regression Analysis	350–1000 (25 Feature Wavelength)	16	0.253	0.889	0.826	0.793	0.828
	1000–1700 (13 Feature Wavelength)	13	0.320	0.792	0.810	0.714	0.643

Note: The bolded part is the best parameter.

3.3. Construction of Lamb/Non-Lamb Identification Model

Pure lamb samples were taken as the lamb group, and samples of lamb mixed with other meat were classified as the non-lamb group (adulterated lamb). A lamb/non-lamb qualitative identification model was then constructed. For this model, samples within the 450–1000 nm range were randomly divided into a calibration set (270 samples) and a prediction set (89 samples). Similarly, samples within the 1000–1400 nm range were also

randomly divided into corresponding sets. The original spectra of these samples underwent various preprocessing steps, including 15-point smoothing, first derivative, second derivative, standard normal variate (SNV) transformation, multiplicative scatter correction (MSC), as well as combinations of first derivative + SNV and second derivative + MSC. The partial least squares discriminant analysis (PLSDA) method was employed for modeling.

In general, an optimal model should have fewer principal components to reduce the dimensionality of data operation. Additionally, the coefficient of determination (R^2) should be greater than 0.9 with values closer to 1 indicating a better fit. Smaller root mean square error of cross-validation (RMSECV) and cross-validation error (Err CV) values suggest a lower error in cross-validation, excluding the possibilities of underfitting or overfitting. A high identification rate is the ultimate criterion for selecting the final model [4,12]. The analysis of the results, presented in Table 4, shows that the optimal model within the 450–1000 nm range is the one preprocessed with the first derivative and SNV, containing seven principal components. This model achieves a 100% identification rate for both lamb and non-lamb groups. For the lamb group, the RMSECV, Err CV, and R^2 values are 0.153, 0.002, and 0.916, respectively. Within the 1000–1400 nm range, the optimal model, also preprocessed with the first derivative and SNV, contains four principal components and achieves a 100% identification rate for both groups. However, for the lamb group, the RMSECV, Err CV, and R^2 values are 0.261, 0.017, and 0.707, respectively. These results indicate that the stability and resolution of the visible-near infrared interval model within the 450–1000 nm range are superior to those within the 1000–1400 nm range.

Table 4. Lamb/non-lamb identification models.

Wavelength (nm)	Preprocessing	Factors	R^2_c	Pure Lamb Group		Prediction Sensitivity of Pure Lamb/%	Prediction Sensitivity of Non-Lamb/%
				Err CV	RMSECV		
450–1000	Smoothing (15)	8	0.795	0.007	0.196	95.0	97.1
	1st der	7	0.891	0.002	0.172	100.0	100.0
	2nd der	7	0.876	0.010	0.217	100.0	97.1
	SNV	7	0.841	0.000	0.176	100.0	98.6
	MSC	7	0.841	0.000	0.176	100.0	98.6
	1st der + SNV	**7**	**0.916**	**0.002**	**0.153**	**100.0**	**100.0**
	1st der + MSC	7	0.912	0.002	0.156	100.0	100.0
1000–1400	Smoothing (15)	10	0.762	0.022	0.235	100.0	98.5
	1st der	10	0.759	0.017	0.238	98.5	100.0
	2nd der	12	0.805	0.017	0.234	100.0	98.5
	SNV	5	0.773	0.021	0.231	100.0	98.5
	MSC	6	0.804	0.017	0.217	100.0	96.9
	1st der + SNV	**4**	**0.707**	**0.017**	**0.261**	**100.0**	**100.0**
	1st der + MSC	4	0.698	0.017	0.272	100.0	98.5

Note: The bolded part is the best parameter.

For the identification of adulterated lamb, businesses and consumers in the circulation chain terminal only need to determine whether the lamb is adulterated without the need to identify the specific type of adulteration. Therefore, the constructed lamb/non-lamb identification model satisfies the requirements of the meat industry chain terminal. Additionally, considering the lower price of visible near-infrared components, the model leverages visible-near infrared spectrum data to meet the demands of both a high discriminant rate and low cost.

3.4. Construction of Foreign Bodies Kind Identification Model of Adulterated Meat

The experimental samples consisted of four types: pure lamb, lamb adulterated with chicken, lamb adulterated with duck, and lamb adulterated with pork. These samples were randomly divided into 270 calibration sets and 86 prediction sets according to a 3:1 ratio. Various spectral pretreatment methods, combined with the PLS method, were utilized to create models within the Vis-NIR range of 450–1000 nm and the NIR range of 1000–1700 nm. The results are presented in Table 5.

Table 5. Chicken, duck and pork identification models of adulterated meat.

Wavelength (nm)	Preprocessing	Groups	Factors	Cross Validation Sensitivity/%	RMSECV	Prediction Sensitivity/%
450–1000	Smoothing (15)	pure lamb lamb/chicken lamb/duck lamb/pork	11	100.0 96.6 96.0 97.3	0.202 0.210 0.249 0.242	100.0 100.0 100.0 96.0
	1st der	pure lamb lamb/chicken lamb/duck lamb/pork	10	100.0 98.3 96.0 97.3	0.182 0.182 0.218 0.220	100.0 100.0 100.0 100.0
	2nd der	pure lamb lamb/chicken lamb/duck lamb/pork	14	100.0 94.9 97.3 94.7	0.215 0.211 0.226 0.244	100.0 89.5 92.0 96.0
	SNV	pure lamb lamb/chicken lamb/duck lamb/pork	11	100.0 98.3 97.3 98.7	0.155 0.186 0.198 0.186	100.0 100.0 100.0 100.0
	MSC	pure lamb lamb/chicken lamb/duck lamb/pork	11	100.0 98.3 97.3 98.7	0.156 0.186 0.198 0.187	100.0 100.0 100.0 100.0
	1st der + SNV	pure lamb lamb/chicken lamb/duck lamb/pork	10	100.0 98.3 98.7 97.3	0.167 0.182 0.216 0.231	100.0 100.0 100.0 100.0
	1st der + MSC	pure lamb g lamb/chicken lamb/duck lamb/pork	10	100.0 98.3 98.7 96.0	0.171 0.185 0.217 0.233	100.0 100.0 100.0 100.0
1000–1400	Smoothing (15)	pure lamb lamb/chicken lamb/duck lamb/pork	10	98.6 86.0 85.1 77.8	0.239 0.277 0.341 0.343	100.0 94.1 83.3 91.7
	1st der	pure lamb lamb/chicken lamb/duck lamb/pork	10	98.6 80.0 71.6 77.8	0.245 0.280 0.344 0.343	100.0 100.0 75.0 91.7
	2nd der	pure lamb lamb/chicken lamb/duck lamb/pork	11	98.6 82.0 82.4 83.3	0.237 0.261 0.351 0.329	100.0 94.1 70.8 91.7
	SNV	Pure lamb lamb/chicken lamb/duck lamb/pork	7	98.6 90.0 75.7 80.6	0.238 0.312 0.461 0.428	100.0 94.1 79.2 87.5
	MSC	pure lamb lamb/chicken lamb/duck lamb/pork	7	98.6 90.0 75.7 81.9	0.243 0.313 0.467 0.430	100.0 94.1 79.2 87.5
	1st der + SNV	pure lamb lamb/chicken lamb/duck lamb/pork	13	98.6 86.0 85.1 91.7	0.447 0.476 0.424 0.746	100.0 100.0 83.3 91.7
	1st der + MSC	pure lamb lamb/chicken lamb/duck lamb/pork g	12	98.6 84.0 86.5 91.7	0.465 0.434 0.438 0.636	100.0 100.0 83.3 87.5

In the 450–1000 nm range, selecting 10 or 11 principal factors, models using most pretreatment methods could effectively distinguish between the groups with the excep-

tion of the second derivative. The optimal model employed the first derivative + SNV pretreatment method, selecting 10 principal factors. This model achieved a 100% identification rate for both the adulterated and pure lamb groups. During cross-validation, the identification rates for the adulterated lamb groups (chicken, duck, and pork) were 98.3%, 98.7%, and 98.3%, respectively, which were higher than those of other models. Additionally, the RMSECV for all groups was below 0.25. In the 1000–1400 nm range, while ensuring a high identification rate, the model using the first derivative + SNV pretreatment method was optimal. With 13 principal factors, the model achieved a 100% identification rate for the pure lamb and chicken adulteration groups in the prediction set, 83.3% for the duck adulteration group, and 91.7% for the pork adulteration group. During cross-validation, the identification rates were 98.6% for pure lamb, 86.0% for chicken adulteration, 85.1% for duck adulteration, and 91.7% for pork adulteration.

Upon comparing the models built within the two wavelength ranges, it was observed that in the near-infrared range of 1000–1400 nm, the identification rate for the adulterated groups did not exceed 90% simultaneously. Notably, the identification rate for the duck adulterated group was lower than that of the other groups with only 83.3% in the optimal model. Furthermore, the RMSECV for each group in the 1000–1400 nm model was higher than that of the 450–1000 nm model, indicating that the model within the 450–1000 nm range exhibited better prediction ability and higher stability.

In conclusion, within the 450–1000 nm range, using the first derivative + SNV as the pretreatment method, the PLS model constructed with 10 main factors was more effective in detecting the type of adulterated meat (chicken, duck, pork) or determining if it was pure lamb.

3.5. Construction of Quantitative Prediction Model for Adulteration of Lamb

The quantitative prediction models for lamb mixed with chicken and duck are described as follows. The model for lamb mixed with chicken consists of 98 samples with varying proportions of chicken included. Specifically, 74 samples are used in the calibration set, and 24 samples are used in the prediction set. Similarly, the model for lamb mixed with duck comprises 120 mixed samples, which are divided into 90 samples for the calibration set and 30 samples for the prediction set. The distribution and number of samples in these sets are consistent with those in the pork adulteration model. The optimal parameters for all three PLSR models are presented in Table 6.

Table 6. The optimum models for adulteration of lamb (chicken, duck and pork) in 450–1000 nm.

Optimum Models	Optimum Preprocessing	PC Number	R^2c	RMSEC	RMSECV	R^2p	RMSEP
Adulterated with chicken	1st der + SNV	6	0.991	0.031	0.052	0.972	0.054
Adulterated with duck	SNV	8	0.994	0.023	0.042	0.985	0.040
Adulterated with pork	MSC	10	0.997	0.018	0.040	0.981	0.044

In the quantitative models, RMSECV typically decreases as the number of principal factors increases, which is followed by a slight increase and then a continued decrease. The fluctuation in RMSECV later on is attributed to the inclusion of background noise in the modeling due to the addition of more principal factors, which is undesirable even if the fitting effect is satisfactory [41]. Therefore, the minimum RMSECV value observed during the first reduction is chosen as the optimal number of principal factors. By comparing the best principal factor models derived from different pretreatment methods, the optimal quantitative model can be obtained. For the quantitative prediction model of lamb mixed with varying proportions of chicken, the combination of the first derivative and Standard Normal Variate (SNV) preprocessing is employed. The correlation coefficients (R^2c and R^2p) for the calibration and prediction sets are 0.991 and 0.972, respectively. The root mean square errors for the calibration set, prediction set, and cross-validation set are 0.031, 0.054,

and 0.052, respectively (Figure 4). Similarly, for the model of lamb mixed with varying proportions of duck, SNV preprocessing is used. The R^2c and R^2p for the calibration and verification sets are 0.994 and 0.985, respectively, with RMSEC, RMSEP, and RMSECV values of 0.023, 0.040, and 0.042, respectively (Figure 5). The pork adulteration quantitative model utilizes the MSC method, yielding R^2c and R^2p values of 0.997 and 0.981 for the calibration and verification sets, respectively, with RMSEC, RMSEP, and RMSECV values of 0.018, 0.044, and 0.040, respectively (Figure 6). These three adulteration quantitative models exhibit high accuracy and stability, demonstrating good prediction capabilities for adulteration in unknown samples.

Figure 4. Quantitative prediction model of adulterated chicken in lamb. The green line represents the trend line of the predicted value of the correction set, and the red line represents the trend line of the true value of the correction set.
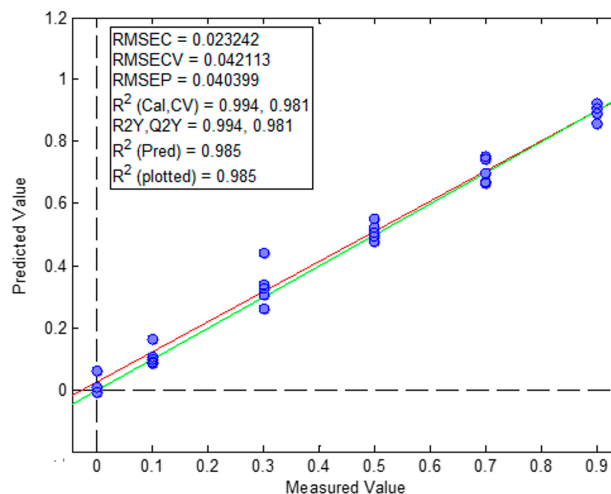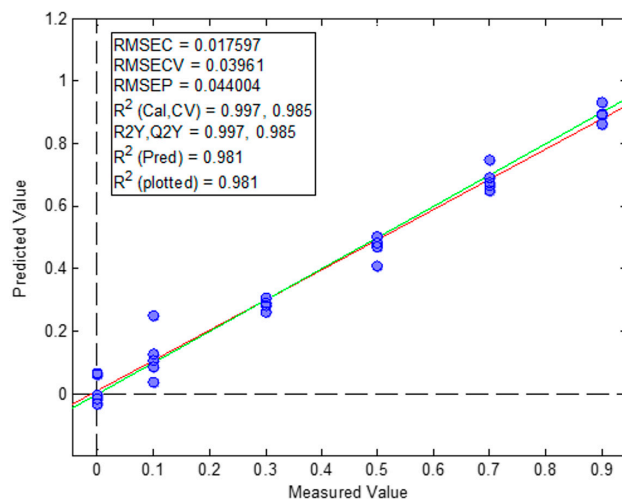

Figure 5. Quantitative prediction model of adulterated duck in lamb. The green line represents the trend line of the predicted value of correction set, and the red line represents the trend line of the true value of the correction set.

Figure 6. Quantitative prediction model of adulterated pork in lamb. The green line represents the trend line of the predicted value of the correction set, and the red line represents the trend line of the true value of the correction set.

When comparing the performance of the models developed in this study to existing literature, significant improvements and novel insights are evident. Previous studies, such as Cozzolino [36] in 2004, utilized visible and near-infrared spectroscopy to distinguish muscle samples of cattle, sheep, pigs, and chickens, achieving an accuracy of 80% using the partial least squares method for qualitative analysis. However, this study not only achieves higher accuracy but also provides quantitative predictions for adulteration levels within a broader range (0–90%). Alamprese et al. [3] identified adulterated beef with turkey using UV, NIR, and IR with adulteration levels ranging from 5% to 50%. Their UV-visible model had an average prediction accuracy of 54.6% for beef adulteration levels of 0–50%, with a cross-validation accuracy of 71.3%, while the near-infrared and infrared models had average prediction accuracies of 71.2% and 65.2%, respectively. In contrast, NIR-based models in this study demonstrate superior performance with cross-validation sensitivities of 100% for pure lamb, 98.3% for chicken adulteration, 98.7% for duck adulteration, and 97.3% for pork adulteration. Furthermore, this study introduces new insights by comparing different pretreatment methods and models, ultimately identifying the optimal combination for each type of adulteration. These findings emphasize the novelty and impact of this work in improving adulteration detection using NIR spectroscopy.

Furthermore, Liang et al. [42] used near-infrared spectroscopy technology combined with orthogonal partial least squares discriminant analysis (OPLS-DA) to identify chicken and duck meat mixed in beef and mutton. They found that through specific preprocessing methods, the identification accuracy of the model can be significantly improved, providing an effective means for the rapid detection of meat adulteration. The study by Fengou et al. [43] used multispectral imaging (MSI) technology combined with support vector machine (SVM) classification to detect the adulteration of pork and chicken in different states (fresh, stored, cooked). Their research showed that the combination of MSI and SVM has high potential in quickly identifying adulterated meat samples with accuracy rates exceeding 93%. Feng et al. [44] conducted a detailed analysis of chicken adulteration in chilled mutton using NIR spectroscopy. They employed a comprehensive approach, including spectral preprocessing, feature wavelength extraction, and modeling using PLS and support vector machines (SVMs). Their study, which focused on samples with different fat-to-lean ratios, achieved remarkable results. Ainara et al. [25] employed NIRS and PCA and PLS-DA to identify meat adulteration in minced lamb and beef, and the research achieved high classification accuracies of 78.95% to 100%. Their study highlighted the effectiveness of NIRS and PLS-DA in detecting meat fraud, especially for pork, Lidia breed cattle, and foal meat at 2% and 1% levels or higher. Compared with these studies, this study

not only covers the detection of adulteration in chicken and duck meat but also includes pork, which is more common in the market. In addition, dual band spectral acquisition was used to provide richer information for the model. This study expanded the scope of analysis to include a wider range of adulterants and concentrations, enhancing the robustness of our model; the model constructed in this study achieved 100% validation set accuracy in identifying pure and adulterated lamb meat, which is leading in existing research. These improvements indicate that this study has made significant progress in improving the accuracy and applicability of meat adulteration detection.

4. Conclusions

In this study, three kinds of models at different levels were constructed at 350–1000 nm to identify adulterated lamb and obtain the best results. The lamb/non-lamb identification model applied at the end of the industrial chain can accurately judge whether the sample is lamb or not. For the adulterated lamb with chicken, duck and pig at any proportion, the identification rate of the optimal model reaches 100%, which is the first-order derivative + SNV data processing method with seven main factors and an RMSECV of 0.153. The foreign bodies identification model of adulterated meat is used in the preliminary prediction of mass testing for quality inspection institutions. The identification model that can well distinguish the species of adulterated meat (chicken, duck and pork) adopts the first-order derivative + SNV data processing method with 10 main factors. The cross-identification rates of adulteration of chicken, duck and pork were 98.3%, 98.7% and 97.3%, respectively. After determining the adulteration meat was chicken, duck or pig, sometimes it is necessary to further quantify the proportion of adulteration. Three quantitative prediction models adopted first-order derivative + SNV, SNV and MSC pretreatment methods, respectively, and selected 6, 8 and 10 factors. Under these conditions, the correlation coefficients (Rp) for the prediction model of chicken, duck and pork adulterated lamb were 0.972, 0.985 and 0.981, respectively.

The experimental results show that using spectral technology combined with model construction technology can effectively identify adulterated lamb and accurately predict the adulteration ratio. However, this study also has certain limitations, such as the experimental samples mainly coming from specific regions, which may not fully represent all types of lamb meat and their adulteration in the market. In the future, sample sources and quantities can be expanded to improve the generalization ability and applicability of the model. In-depth research can be conducted on spectral data preprocessing and feature wavelength screening methods to further optimize the model structure, improving prediction accuracy and stability. This study will help promote the development of quality control technology for meat products, safeguarding consumer rights and the market order.

References

1. Available online: https://data.stats.gov.cn/easyquery.htm?cn=C01 (accessed on 1 September 2024).
2. Ballin, N.Z. Authentication of meat and meat products. *Meat Sci.* **2010**, *86*, 577–587. [CrossRef] [PubMed]
3. Alamprese, C.; Casale, M.; Sinelli, N.; Lanteri, S.; Casiraghi, E. Detection of minced beef adulteration with turkey meat by UVevis, NIR and MIR spectroscopy. *LWT Food Sci. Technol.* **2013**, *53*, 225–232. [CrossRef]
4. Zheng, X.C.; Li, Y.Y.; Wei, W.S.; Peng, Y. Detection of adulteration with duck meat in minced lamb meat by using visible near-infrared hyperspectral imaging. *Meat Sci.* **2019**, *149*, 55–62. [CrossRef]
5. Ong, S.B.; Zuraini, M.I.; Jurin, W.G.; Jurin, Y.K.; Cheah, R.; Tunung, L.C.; Chai, Y.; Haryani, F. Meat molecular detection: Sensitivity of polymerase chain reaction-restriction fragment length polymorphism in species differentiation of meat from animal origin. *ASEAN Food J.* **2007**, *14*, 51–59.
6. Li, T.T.; Jalbani, Y.M.; Zhang, G.L.; Zhao, Z.Y.; Wang, Z.Y.; Zhao, X.Y.; Chen, A.L. Detection of goat meat adulteration by real-time PCR based on a reference primer. *Food Chem.* **2019**, *277*, 554–557. [CrossRef]
7. Perestam, A.T.; Fujisaki, K.K.; Nava, O.; Hellberg, R.S. Comparison of real-time PCR and ELISA-based methods for the detection of beef and pork in processed meat products. *Food Control* **2017**, *71*, 346–352. [CrossRef]
8. Jiang, X.; Rao, Q.; Mittl, K.; Hsieh, Y.-H.P. Monoclonal antibody-based sandwich ELISA for the detection of mammalian meats. *Food Control* **2020**, *10*, 107045. [CrossRef]
9. Orduna, A.R.; Husby, E.; Yang, C.T.; Ghosh, D.; Beaudry, F. Detection of meat species adulteration using high-resolution mass spectrometry and a proteogenomics strategy. *Food Addit. Contam.* **2017**, *34*, 1110–1120. [CrossRef]
10. Li, Y.; Zhang, Y.; Li, H.; Zhao, W.; Guo, W.; Wang, S. Simultaneous determination of heat stable peptides for eight animal and plant species in meat products using UPLC-MS/MS method. *Food Chem.* **2018**, *245*, 125–131. [CrossRef]
11. Ross, A.; Brunius, C.; Chevallier, O.; Dervilly, G.; Elliott, C.; Guitton, Y.; Prenni, J.E.; Savolainen, O.; Hemeryck, L.; Vidkjær, N.H.; et al. Making complex measurements of meat composition fast: Application of rapid evaporative ionisation mass spectrometry to measuring meat quality and fraud. *Meat Sci.* **2021**, *181*, 10833. [CrossRef]
12. Kamruzzaman, M.; Sun, D.W.; Elmasry, G.; Allen, P. Fast detection and visualization of minced lamb meat adulteration using NIR hyperspectral imaging and multivariate image analysis. *Talanta* **2013**, *103*, 130–136. [CrossRef]
13. Kamruzzaman, M.; Haque, M.E.; Ali, M.R. Hyperspectral imaging technique for offal quantification in minced meat. *J. Bangladesh Agric.* **2014**, *12*, 189–194. [CrossRef]
14. Ropodi, A.I.; Pavlidis, D.E.; Mohareb, F.; Panagou, E.; Nychas, G.-J. Multispectral image analysis approach to detect adulteration of beef and pork in raw meats. *Food Res. Int.* **2015**, *67*, 12–18. [CrossRef]
15. Kamruzzaman, M.; Makino, Y.; Oshita, S. Rapid and non-destructive detection of chicken adulteration in minced beef using visible near-infrared hyperspectral imaging and machine learning. *J. Food Eng.* **2016**, *170*, 8–15. [CrossRef]
16. *GB/T 38164-2019*; Common Methods for Detecting Animal Derived Components in Livestock and Poultry, Real-Time Fluorescence PCR Method. Chinese Standard: Beijing, China, 2019.
17. *GB/T 35918-2018*; Gene Barcode Technology for Animal Origin Detection in Animal Products, Sanger Sequencing Method. Chinese Standard: Beijing, China, 2018.
18. Qu, F.; Ren, D.; He, Y.; Nie, P.; Lin, L.; Cai, C.; Dong, T. Predicting pork freshness using multi-index statistical information fusion method based on near infrared spectroscopy. *Meat Sci.* **2018**, *146*, 59–67. [CrossRef]
19. Kapper, C.; Klont, R.E.; Verdonk, J.M.A.J.; Williams, P.C.; Urlings, H.A.P. Prediction of pork quality with near infrared spectroscopy (NIRS) 2. Feasibility and robustness of NIRS measurements under production plant conditions. *Meat Sci.* **2012**, *91*, 300–305. [CrossRef]
20. Mahmoud, A.S.; Marlon, M.R.; Qi, Y.W.; Klette, R. Detection of Red-Meat Adulteration by Deep Spectral–Spatial Features in Hyperspectral Images. *J. Imaging.* **2018**, *4*, 2–20.
21. Leng, T.; Li, F.; Xiong, L.; Xiong, Q.; Zhu, M.; Chen, Y. Quantitative detection of binary and ternary adulteration of minced beef meat with pork and duck meat by NIR combined with chemometrics. *Food Control* **2020**, *113*, 107203. [CrossRef]
22. Wang, P.P. *Study on the Breed Discrimination and Quality Determination of Lamb by Near Infrared Spectroscopy*; Institute of Agricultural Products Processing, Chinese Academy of Agricultural Sciences: Beijing, China, 2012.
23. Dixit, Y.; Casado-Gavalda, M.P.; Cama-Moncunill, R.; Cama-Moncunill, X.; Markiewicz-Kęszycka, M.; Cullen, P.J.; Sullivan, C. Developments and challenges in online NIR spectroscopy for meat processing. *Compr. Rev. Food Sci. Food.* **2017**, *16*, 1172–1187. [CrossRef]
24. Savoia, S.; Albera, A.; Brugiapaglia, A.; Di Stasio, L.; Ferragina, A.; Cecchinato, A.; Bittante, G. Prediction of meat quality traits in the abattoir using portable and hand-held near-infrared spectrometers. *Meat Sci.* **2020**, *161*, 108017. [CrossRef]
25. López-Maestresalas, A.; Insausti, K.; Jaren, C.; Pérez-Roncal, C.; Urrutia, O.; Beriain, M.J.; Arazuri, S. Detection of minced lamb and beef fraud using NIR spectroscopy. *Food Control* **2019**, *98*, 465–473. [CrossRef]
26. Jiang, H.; Yoon, S.C.; Zhuang, H.; Wang, W.; Yang, Y. Evaluation of factors in development of Vis/NIR spectroscopy models for discriminating PSE, DFD and normal broiler breast meat. *Br. Poult. Sci.* **2017**, *6*, 673–680. [CrossRef] [PubMed]
27. Mamani-Linares, L.W.; Gallo, C.; Alomar, D. Identification of cattle, llama and horse meat by near infrared reflectance or transflectance spectroscopy. *Meat Sci.* **2012**, *90*, 378–385. [CrossRef] [PubMed]
28. Weng, S.; Guo, B.; Tang, P.; Yin, X.; Pan, F.; Zhao, J.; Huang, L.; Zhang, D. Rapid detection of adulteration of minced beef using Vis/NIR reflectance spectroscopy with multivariate methods. *Spectrochim. Acta Part A* **2020**, *230*, 118005. [CrossRef] [PubMed]

29. *SB/T 11093-2014*; Ministry of Commerce Market Operation Department, Ministry of Commerce Circulation Industry Promotion Center, Huashan Reserves Commodity Management Center; Central Reserve Frozen Rolled Mutton [Standard]. Ministry of Commerce, Vanijya Bhawan: New Delhi, India, 2014.

30. Bonin, M.D.N.; Silva, S.D.L.E.; Bünger, L.; Ross, D.; Feijó, G.L.D.; Gomes, R.d.C.; Rennó, F.P.; Santana, M.H.d.A.; de Rezende, F.M.; Ítavo, L.C.V.; et al. Predicting the shear value and intramuscular fat in meat from Nellore cattle using Vis-NIR spectroscopy. *Meat Sci.* **2020**, *163*, 108077.

31. Kamruzzaman, M.; Makino, Y.; Oshita, S.; Liu, S. Assessment of Visible Near-Infrared Hyperspectral Imaging as a Tool for Detection of Horsemeat Adulteration in Minced Beef. *Food Bioprocess Technol.* **2015**, *8*, 1054–1062. [CrossRef]

32. Barbina, D.F.; ElMasrya, G.; Suna, D.W.; Allen, P. Predicting quality and sensory attributes of pork using near-infrared hyperspectral imaging. *Anal. Chim. Acta* **2012**, *719*, 30–42. [CrossRef]

33. Zhang, Y.D.; Xue, H.T.; Ma, Q.Y.; Li, Y.; Zhou, Q.; Sun, J.; Wang, W. Potential of two-dimensional correlation-based dual-band visible/near infrared spectroscopy to predict total volatile basic nitrogen content in meat. *J. Food Compos. Anal.* **2024**, *133*, 106451. [CrossRef]

34. An, J.Y.; Li, Y.L.; Zhang, C.Z.; Zhang, D. Rapid nondestructive prediction of multiple quality attributes for different commercial meat cut types using optical system. *Food Sci. Anim. Resour.* **2022**, *42*, 655–671. [CrossRef]

35. Sahar, A.; Allen, P.; Sweeney, T.; Cafferky, J.; Downey, G.; Cromie, A.; Hamill, M.R. Online Prediction of Physico-Chemical Quality Attributes of Beef Using Visible—Near-Infrared Spectroscopy and Chemometrics. *Foods* **2019**, *8*, 525. [CrossRef]

36. Cozzolinoa, D.; Murray, I. Identification of animal meat muscles by visible and near infrared reflectance spectroscopy. *LWT Food Sci. Technol.* **2004**, *37*, 447–452. [CrossRef]

37. Huang, K.P. Study on the Parameters of Mutton Freshness by Near Infrared Spectroscopy. Ph.D. Thesis, Shihezi University, Xinjiang, China, 2017.

38. Lu, Y.X.; Zhai, R.; Wu, F. Research progress on detection technology of meat adulteration. *Acta Metrol. Sin.* **2003**, *44*, 1000–1008.

39. Pu, H.; Sun, D.W.; Ma, J. Hierarchical variable selection for predicting chemical constituents in lamb meats using hyperspectral imaging. *J. Food Eng.* **2014**, *143*, 44–52. [CrossRef]

40. Kademi, H.I.; Ulusoy, B.H.; Hecer, C. Applications of Miniaturized and Portable Near Infrared Spectroscopy (NIRS) for Inspection and Control of Meat and Meat Products. *J. Food Eng.* **2019**, *35*, 201–220. [CrossRef]

41. Fan, Y.X. Rapid Detection of Minced Pork Quality and Safety Based on Visible and Near Infrared Spectroscopy. Master's Thesis, Zhejiang University, Hangzhou, China, 2011.

42. Liang, J.; Hao, S.Y.; Zhao, X.M.; Li, L.L.; Kang, J.; Nian, F.; Zhang, Z.J.; Tang, D.F. Construction of an adulteration identification model for beef and mutton based on near-infrared spectroscopy. *J. Gansu Agri. Univ.* **2023**, *1*, 19–29.

43. Fengou, L.C.; Panagiotis, T.; George-John, E.N. Rapid Detection of Minced Pork and Chicken Adulteration in Fresh, Stored and Cooked Ground Meat. *Food Control* **2021**, *125*, 108002. [CrossRef]

44. Feng, J.X.; Li, Z.G.; Zhang, X.S. Identification and analysis of chicken adulteration in chilled mutton by near-infrared spectroscopy. *Food Sci. Technol.* **2022**, *47*, 284–290.